Mineralogical Magazine (2021), **85**, 142–148
doi:10.1180/mgm.2020.98

CAMBRIDGE UNIVERSITY PRESS

Article

Galeaclolusite, $[Al_6(AsO_4)_3(OH)_9(H_2O)_4]\cdot 8H_2O$, a new bulachite-related mineral from Cap Garonne, France

Ian E. Grey[1]*, George Favreau[2], Stuart J. Mills[3], W. Gus Mumme[1], Catherine Bougerol[4], Helen E.A. Brand[5], Anthony R. Kampf[6], Colin M. MacRae[1] and Finlay Shanks[7]

[1]CSIRO Mineral Resources, Private Bag 10, Clayton South, Victoria 3169, Australia; [2]421 avenue Jean Monnet, 13090 Aix-en-Provence, France; [3]Geosciences, Museums Victoria, GPO Box 666, Melbourne, Victoria 3001, Australia; [4]Université Grenoble Alpes and CNRS, Institut Néel, 38000, Grenoble, France; [5]Australian Synchrotron, 800 Blackburn Road, Clayton, Victoria 3168, Australia; [6]Mineral Sciences Department, Natural History Museum of Los Angeles County, 900 Exposition Boulevard, Los Angeles, CA90007, USA; and [7]School of Chemistry, Monash University, Clayton, Victoria 3800, Australia.

Abstract

Galeaclolusite, $[Al_6(AsO_4)_3(OH)_9(H_2O)_4]\cdot 8H_2O$, is a new secondary hydrated aluminium arsenate mineral from Cap Garonne, Var, France. It forms crusts and spheroids of white fibres up to 50 μm long by 0.4 μm wide and only 0.1 μm thick. The fibres are elongated along [001] and flattened on (100). The calculated density is 2.27 g·cm^{-3}. Optically, galeaclolusite is biaxial with $\alpha = 1.550(5)$, β not determined, $\gamma = 1.570(5)$ (white light) and partial orientation: $Z = \mathbf{c}$ (fibre axis). Electron microprobe analyses coupled with crystal structure refinement results gives an empirical formula based on 33 O atoms of $Al_{5.72}Si_{0.08}As_{2.88}O_{33}H_{34.12}$. Galeaclolusite is orthorhombic, *Pnma*, with $a = 19.855(4)$, $b = 17.6933(11)$, $c = 7.7799(5)$ Å, $V = 2733.0(7)$ Å^3 and $Z = 4$. The crystal structure of galeaclolusite was established from its close relationship to bulachite and refined using synchrotron powder X-ray diffraction data. It is based on heteropolyhedral layers, parallel to (100), of composition $Al_6(AsO_4)_3(OH)_9(H_2O)_4$ and with H-bonded H_2O between the layers. The layers contain [001] spiral chains of edge-shared octahedra, decorated with corner-connected AsO_4 tetrahedra, that are the same as in the mineral liskeardite.

Keywords: bulachite, galeaclolusite, new mineral, Cap Garonne, crystal structure, synchrotron

(Received 7 October 2020; accepted 30 November 2020; Accepted Manuscript published online: 4 December 2020; Associate Editor: Oleg I Siidra)

Introduction

Bulachite, from Neubulach, in the Black Forest region, Germany, was first described by Walenta (1983) as having the ideal formula $Al_2(AsO_4)(OH)_3(H_2O)_3$ and orthorhombic symmetry with unit cell parameters $a = 15.53$, $b = 17.78$ and $c = 7.03$ Å. The mineral occurs as surface coatings of white, ultrathin fibres. The structure remained undetermined until recently, when application of the low-dose electron diffraction tomography technique coupled with synchrotron powder X-ray diffraction (PXRD) established the correct formula and unit cell as $[Al_6(AsO_4)_3(OH)_9(H_2O)_4]\cdot 2H_2O$ with $a = 15.3994(3)$, $b = 17.6598(3)$, $c = 7.8083(1)$ Å and space group *Pnma* (Grey *et al.*, 2020b). The structure is based on heteropolyhedral layers, parallel to (100), of composition $Al_6(AsO_4)_3(OH)_9(H_2O)_4$ and with H-bonded H_2O between the layers. The layers contain [001] spiral chains of edge-shared octahedra, decorated with corner connected AsO_4 tetrahedra, that are the same as in the mineral liskeardite (Grey *et al.*, 2013).

In the course of our ongoing study of the structure and chemistry of minerals from the Cap Garonne copper mine (Favreau and Galea-Clolus, 2014; Grey *et al.*, 2014; Mills *et al.*, 2014, 2015, 2017, 2018, 2019; Plášil *et al.*, 2018), one of us (G.F.) located fibrous coatings of a white mineral for which energy-dispersive X-ray analysis gave the same composition as reported for bulachite (Walenta, 1983). A PXRD pattern for the mineral had a number of sharp peaks in common with those for bulachite, but the pattern did not contain the strongest bulachite peak at 7.78 Å and it contained several broad peaks not present in the Walenta (1983) pattern, with the strongest peak being at $d \approx 10$ Å. Electron diffraction (ED) patterns obtained on individual fibres enabled the PXRD pattern to be indexed with a unit cell having the same b and c parameters as bulachite, but with a increased to ~19.9 Å. Thermo-crystallographic studies on the Cap Garonne specimen (Grey *et al.*, 2020b) showed that the PXRD pattern started transforming to that for bulachite at ~50°C and the transformation was complete above 75°C. This suggested that the Cap Garonne mineral was a higher hydrate with a layer structure related to the bulachite structure, so that mild heating results in loss of interlayer water accompanied by a large decrease in the interlayer separation along [100]. On this basis, a structural model was developed for the higher hydrate and refined using synchrotron PXRD data, leading to the development of a mineral naming proposal.

The new mineral and its name, galeaclolusite, were approved by the Commission on New Minerals, Nomenclature and Classification (CNMNC) of the International Mineralogical Association (IMA2020–052, Grey *et al.*, 2020a). The name is for

*Author for correspondence: Ian E. Grey, Email: ian.grey@csiro.au
Cite this article: Grey I.E., Favreau G., Mills S.J., Mumme W.G., Bougerol C., Brand H.E.A., Kampf A.R., MacRae C.M. and Shanks F. (2021) Galeaclolusite, $[Al_6(AsO_4)_3(OH)_9(H_2O)_4]\cdot 8H_2O$, a new bulachite-related mineral from Cap Garonne, France. *Mineralogical Magazine* **85**, 142–148. https://doi.org/10.1180/mgm.2020.98

Valérie Galea-Clolus (born 18 November 1964) in recognition of her significant contributions to Cap Garonne mineralogy. She was President of the AAMCG (Friends of the mine) for many years and co-author of a book on the mine (Favreau and Galea-Clolus, 2014). She was the first to map the uranium-rich zones and has found several new minerals and polytypes at the mine (e.g. gobelinite, Mills *et al.*, 2020). Importantly, she has encouraged dissemination of the mineralogy of Cap Garonne through the museum and public outreach as well as making scientific inspection of the mine possible. The holotype sample is housed in the mineralogical collections at Museums Victoria, GPO Box 666, Melbourne, Victoria 3001, Australia, registration number M55455. A cotype used for optical measurements is in the collections of the Natural History Museum of Los Angeles County, 900 Exposition Boulevard, Los Angeles, CA 90007, USA with catalogue number 74874.

Occurrence and paragenesis

Specimens of galeaclolusite were collected in Salle B, South mine, Cap Garonne, Var, France (43°4′53″N, 6°1′55″E; Favreau and Galea-Clolus, 2014), close to a uranium-rich zone which yielded the type specimen of deloryite (Sarp and Chiappero, 1992). It occurs most commonly as patchy white crusts on yellow bariopharmacoalumite-*Q*2*a*2*b*2*c* (Grey *et al.*, 2014, 2020b). Needle-like crystals of galeaclolusite are associated intimately with needles of bulachite in the crusts, with the latter localised at the surface of the crusts. In better crystallised specimens, it is present as small spheroids of radiating blades (Fig. 1). Other associated minerals are green cubes of bariopharmacosiderite, olivenite, pyrite and strongly etched mansfieldite.

Galeaclolusite has probably formed from supergene alteration, with mansfieldite, $Al(AsO_4)\cdot 2H_2O$, providing the elements Al and As, because mansfieldite occurrences close to galeaclolusite at Cap Garonne are deeply etched. Frau and Da Pelo (2001) have previously suggested that mansfieldite may be the source mineral for bulachite formation at Sa Bidda Beccia, southern Sardinia. Alternatively, galeaclolusite may have formed from alteration of bariopharmacoalumite, as evidenced by Fig. 2, showing fine needles of galeaclolusite growing out from fractured cubes of the bariopharmacoalumite.

Fig. 1. Spheroids of galeaclolusite on bariopharmacoalumite. Field of view: 0.55 mm, photo Vincent Bourgoin, Museums Victoria specimen number M55455.

Fig. 2. SEM back-scattered electron image of galeaclolusite fibres protruding from fractured cubes of bariopharmacoalumite. Field of view: 20 μm. Photo Vincent Bourgoin/Association Jean Wyart, Paris, Museums Victoria specimen M52929.

Physical and optical properties

The crusts of galeaclolusite are comprised of small clumps of subparallel ruler-shaped white fibres that are typically up to 50 μm long by 0.4 μm wide and only 0.1 μm thick. Forms are only evident at high magnification in a scanning electron microscope (Fig. 2). The fibres are elongated along [001] and flattened on (100), as determined from transmission electron microscopy and ED. The density could not be measured due to the minute crystal size. The calculated density is 2.27 g·cm^{-3} based on the empirical formula and PXRD cell.

Optically, galeaclolusite is biaxial with the indices of refraction of $\alpha = 1.550(5)$, β not determined, $\gamma = 1.570(5)$ (white light) and partial orientation: $Z = \mathbf{c}$ (fibre axis). The ultrathin character of the galeaclolusite fibres meant that the Becke lines were very difficult to discern, so that the indices of refraction are not well determined, as indicated by their relatively high uncertainties. It was not possible to measure 2V or β, so the optic sign could not be determined. The fibres have parallel extinction and are length slow, as was reported for bulachite (Walenta, 1983). Based on the layer structure and by analogy with bulachite, it is likely that the full optical orientation is $X = \mathbf{a}$, $Y = \mathbf{b}$ and $Z = \mathbf{c}$. The Gladstone–Dale compatibility index (Mandarino, 2007) is −0.003 (superior) based on the empirical formula, calculated density and the average of the indices of refraction α and γ.

Infrared spectroscopy

Attenuated total reflection infrared spectroscopy on clumps of galeaclolusite crystals was conducted using a Bruker Equinox IFS55 spectrometer fitted with Judson MCT detector and Specac diamond ATR. A hundred co-added scans were employed at a spectral resolution of 8 cm^{-1}. The infrared spectrum is shown in Fig. 3. In the OH-stretching region, a broad band has peaks at 2950 and 3425 cm^{-1} with a broad hump between them. The peaks correspond to H-bonded water molecules and hydroxyl ions with O···O H-bonded distances in the range 2.6 to 2.8 Å (Libowitzky, 1999); i.e. of strong to intermediate strength. A band corresponding to H–O–H bending vibrations for water molecules is at 1630 cm^{-1}. The As–O stretching region has a main band at 845 cm^{-1}, with a

https://doi.org/10.1180/mgm.2020.98 Published online by Cambridge University Press

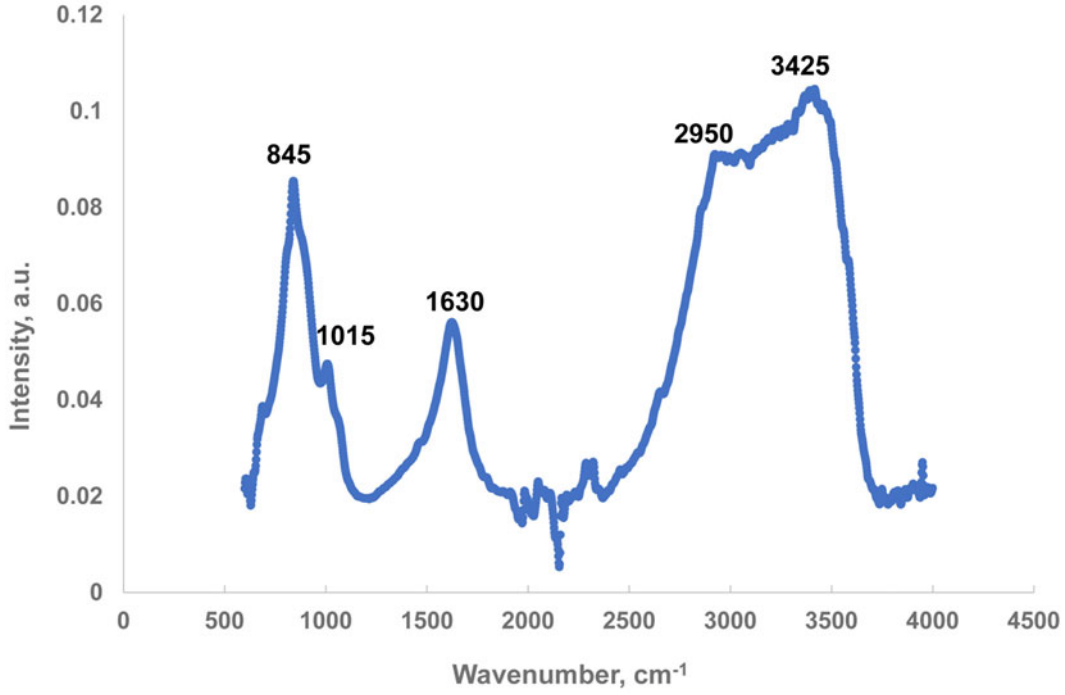

Fig. 3. Infrared spectrum for galeaclolusite. a.u. = arbitrary units

well-defined shoulder at 1015 cm^{-1}. These are within the ranges of metal-coordinated AsO_4 stretching vibrations (Myeni *et al.*, 1998).

Chemical composition

Electron microprobe analyses (EMPA) were made on sectioned and polished clumps of fibres using wavelength-dispersive spectrometry on a JEOL JXA 8500F Hyperprobe operated at an accelerating voltage of 10 kV and a beam current of 4 nA, with a defocused beam of 2 µm. Under these conditions, minimal beam damage was evident after each analysis. Analytical results (average of single analyses of seven dense clumps of fibres) are given in Table 1. The water content is from the crystal structure with 33 O atoms per formula unit. A PAP (Pouchou, 1993) Phi-Rho-Z correction procedure (incorporating *STRATAGem*, Schafer *et al.*, 2018) was employed with oxygen added by stoichiometry. In a separate step, water was considered in the matrix correction. The low analysis total is probably a result of the electron beam interaction volume exceeding the extremely thin (0.1 µm) fibres.

The empirical formula based on 33 O atoms is $Al_{5.72}Si_{0.08}As_{2.88}O_{33}H_{34.12}$. No correlations in chemistry were observed between Al and Si or between As and Si, indicating no isomorphous substitutions of Si. The trace amount of Si in the chemical analysis may represent a surface impurity.

The ideal formula is $[Al_6(AsO_4)_3(OH)_9(H_2O)_4]\cdot 8H_2O$, which requires Al_2O_3 32.28, As_2O_5 36.38, H_2O 31.34, total 100 wt.%.

Crystallography

The galeaclolusite specimens consist of ultrafine fibres (Fig. 2), which were not suitable for single-crystal XRD studies. Information on the unit cell was obtained instead from electron diffraction (ED). Crystal aggregates were sonicated in ethanol and the suspension was dispersed onto a holey carbon grid for transmission electron microscopy (TEM). The TEM studies were conducted using a JEOL 4000EX microscope with a LaB_6 source and a spherical aberration coefficient of 1.06 mm. The microscope was operated at 400 kV, using parallel illumination geometry to minimise beam damage. TEM images were recorded on a Gatan slow scan CCD camera.

Table 1. Analytical data (wt.%) for galeaclolusite.

Constituent	Mean	Range	S.D.	Standard
Al_2O_3	29.7	28.5–32.2	1.3	Berlinite
As_2O_5	33.7	32.2–35.2	1.0	Scorodite
SiO_2	0.5	0.0–1.3	0.4	Wollastonite
H_2O*	31.3			
Total	95.2			

*H_2O from crystal structure; S.D. – standard deviation

The flattened fibres of galeaclolusite all tended to lie flat on the TEM grid, giving the same ED (0*kl*) reciprocal lattice pattern, as shown in figure 4 of Grey *et al.* (2020b). Indexing of the ED pattern gave cell parameters $b = 17.7$ Å and $c = 7.8$ Å, with the direction of the 7.8 Å axis parallel to the fibre length. Systematic absences in the pattern for (0*kl*) reflections with $k + l = 2n + 1$ indicated an *n*-glide plane, with possible space groups *Pnma* or $Pn2_1a$. TEM images confirmed that the direction of the 7.8 Å axis is parallel to the long dimension of the lath. $a = 19.8$ Å, normal to the flattened fibres, was obtained from PXRD by noting enhanced intensity of reflections involving *h* when preferred orientation was accentuated by floating the fibres onto a flat sample holder with ethanol solution.

PXRD data for a crystal structure analysis were collected at the Australian Synchrotron PXRD beamline. Preliminary laboratory PXRD scans showed that even light grinding of the galeaclolusite specimen resulted in loss of long-range ordering (severe peak

https://doi.org/10.1180/mgm.2020.98 Published online by Cambridge University Press

broadening) so, for the synchrotron experiments, small unground clumps of subparallel fibres were packed into a 0.5 mm diameter quartz capillary. A 0.3 mm capillary was then inserted to the edge of the specimen, to prevent any specimen movement during rotation of the capillary. High-energy 21 keV X-rays were used to reduce fluorescence due to As. The wavelength was 0.59028(6) Å, calibrated to NIST standard LaB6 660b. The capillary was positioned in the diffractometer rotation centre and spun at ~1 Hz. The X-ray beam was aligned to coincide with the diffractometer centre and slits were used to restrict the beam width to 2 mm. The data were collected using a Mythen position sensitive detector covering 80° in 2θ with a step size of 0.00375° in 2θ.

Le Bail fitting of the PXRD data to obtain refined unit cell parameters was made using *JANA2006* (Petříček *et al.*, 2014). Manual backgrounds were used with interpolation between 40 points and a pseudo-Voigt peak-shape function. The PXRD pattern for galeaclolusite has complex anisotropic peak broadening. All reflections with non-zero h are broadened and the reflections with h odd are broader than those with h even. This was dealt with by combining anisotropic Lorentzian particle size broadening (parameter LXe) with anisotropic peak broadening for reflections with $h = 2n + 1$. The PXRD data was truncated at 1 Å resolution (peaks were very weak and broad at higher resolution). The LeBail fit gave fit indices of Rp = 2.88, Rwp = 4.06 and GoF = 3.40. The indexed PXRD pattern is given in Table 2 and unit cell parameters refined from the powder data are given in Table 3.

Crystal structure determination and refinement

A model for the crystal structure of galeaclolusite in space group *Pnma* was constructed based on the assumption that it contained the same heteropolyhedral layers as in bulachite (Grey *et al.*, 2020b), with an increased separation between the layers (= 0.5a) from 7.7 Å to 9.9 Å, due to an increased number of interlayer H_2O molecules in galeaclolusite. The x coordinates for the bulachite model were scaled by the ratio of the two a axes to establish the polyhedral layers in the $a = 19.8$ Å galeaclolusite cell. The PXRD pattern for this model was calculated and found to have only a fair agreement with the experimental pattern. We examined the possibility that the difference between the structures of bulachite and galeaclolusite involves not only a change in the interlayer spacing but also a sliding of the layers relative to one another, as we found in studies on other hydrated aluminium arsenate minerals (Grey *et al.*, 2016). In space group *Pnma*, the layers can be displaced relative to one another along [001], with no distortion of the polyhedra, by changing the z coordinate for all atoms by the same amount. We ran a series of tests where the z coordinate for all atoms was changed in increments of 0.01. It was found that changing z in a positive sense improved the fit to the experimental PXRD pattern, and the profile R factors decreased with increasing Δz up to 0.09 then increased with further change in z. The value of Δz was then fixed at 0.09, and difference-Fourier maps were used to locate the interlayer water molecules.

In the Rietveld refinement, the heteropolyhedral layer atomic coordinates derived from the bulachite structure were kept fixed and only group temperature factors (one for water molecules and one for all other atoms) were refined. The profile parameters were refined by Le Bail fitting as described in the previous section. The final agreement factors for the Rietveld fitting of the PXRD data are given in Table 2. The fitted Rietveld pattern is shown in Fig. 4. The atomic coordinates, group B values and bond-valence sums (BVS, Gagné and Hawthorne, 2015) are reported in Table 4. Polyhedral bond distances are given in Table 5. The wide range of Al–O distances (1.85 to 2.05 Å for Al2) is not unusual for hydrated aluminium arsenate minerals (Grey *et al.*, 2013). The crystallographic information file has been deposited

Table 2. Powder X-ray diffraction data for galeaclolusite (d in Å).

I_{obs}	d_{meas}	d_{calc}	h k l
100	**9.973**	**9.927**	**2 0 0**
60	**8.851**	**8.847**	**0 2 0**
36	7.118	7.122	0 1 1
56	**6.696**	**6.704**	**1 1 1**
50	6.617	6.605	2 2 0
38	6.126	6.123	2 0 1
20	5.071	5.070	2 3 0
14	4.701	4.700	0 3 1
18	4.424	4.423	0 4 0
21	3.772	3.775	1 4 1
10	3.565	3.561	0 2 2
74	**3.506**	**3.505**	**1 2 2**
6	3.464	3.468	5 1 1
66	**3.326**	3.333, **3.325**	2 5 0, **3 4 1**
20	3.280	3.284	5 2 1
7	2.922	2.921	0 4 2
8	2.799	2.802	2 4 2
8	2.765	2.762	5 4 1
9	2.653	2.657, 2.650	2 6 1, 6 4 0
2	2.565	2.566	0 1 3
4	2.536	2.535	4 6 0
4	2.508	2.508	6 4 1
12	2.414	2.415, 2.414	3 0 3, 2 2 3
11	2.350	2.350	0 6 2
32	2.334	2.334, 2.329	1 6 2, 3 2 3
16	2.210	2.212	0 8 0
4	2.156	2.155	5 1 3
3	2.106	2.107	1 7 2
5	2.040	2.041	6 0 3
5	2.024	2.025	3 8 1
5	1.946	1.945	0 0 4
4	1.924	1.924, 1.924	1 1 4, 10 0 1
4	1.848	1.846	3 8 2
13	1.774	1.773	1 4 4
2	1.623	1.624	0 6 4
6	1.606	1.605	1 10 2
2	1.546	1.545	1 1 5
5	1.474	1.474	0 12 0

The strongest lines are given in bold

Table 3. Synchrotron PXRD data collection and Rietveld refinement details for galeaclolusite.

Crystal data	
Formula	$[Al_6(AsO_4)_3(OH)_9(H_2O)_4]\cdot 8H_2O$
Unit-cell parameters: a, b, c (Å)	19.855(4), 17.6933(11), 7.7799(5)
Volume (Å^3), Z	2733.0(7), 4
Space group	*Pnma*
Data collection and refinement	
X-ray radiation source, wavelength (Å)	Australian Synchrotron, 0.59028(6)
2θ range, step size (°)	1.50 to 76.32, 0.00375
Resolution for structure analysis (Å), number of contributing reflections	1.0, 1493
Number of profile parameters	8
Number of structural parameters/restraints	2/2
Profile function	Pseudo-Voigt
Background	Interpolation between 40 selected points
R_p, R_{wp}, GoF	5.31, 6.96, 5.83

https://doi.org/10.1180/mgm.2020.98 Published online by Cambridge University Press

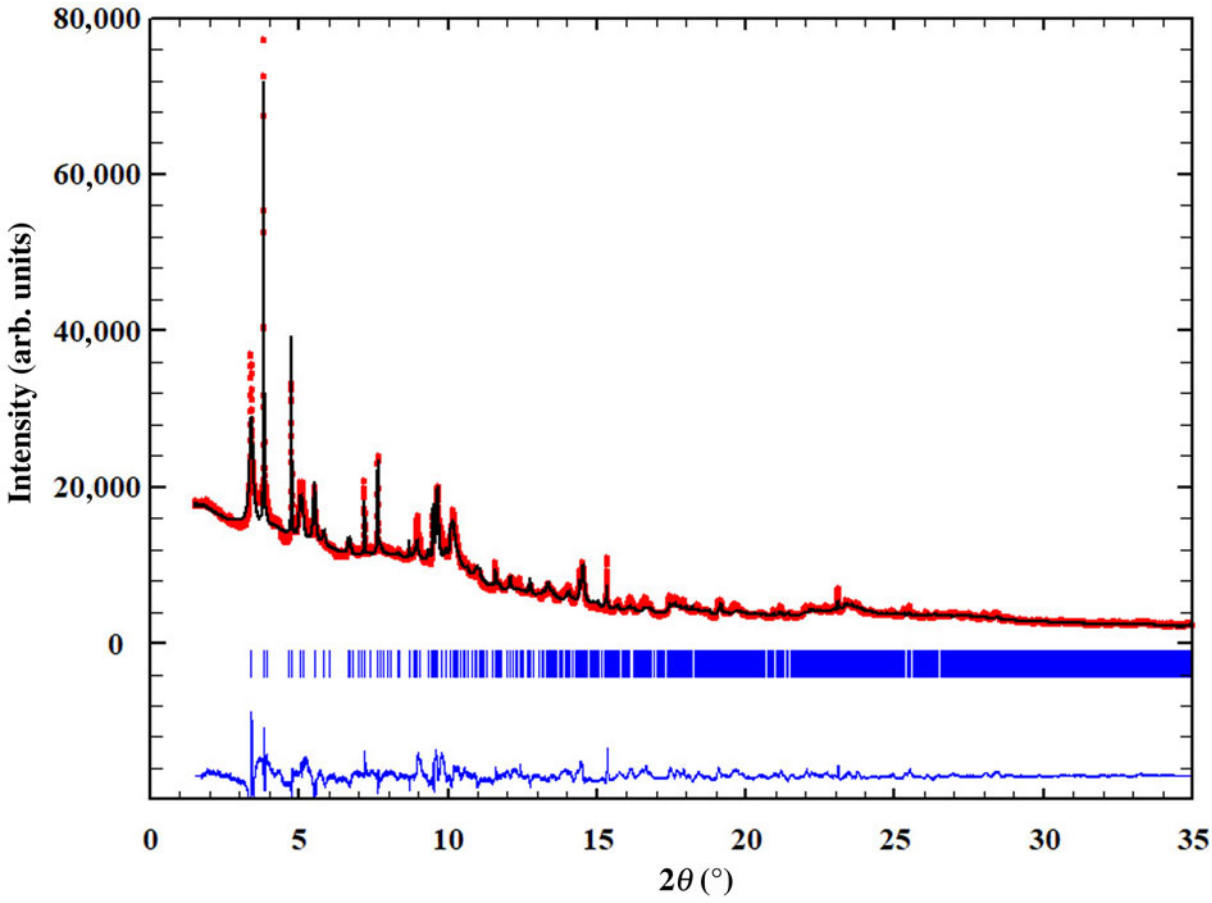

Fig. 4. Rietveld observed (red points) and calculated (black line) PXRD patterns for galeaclolusite from Cap Garonne. Short bars show the positions of the Bragg reflections. The difference plot is in blue.

Table 4. Atomic coordinates, isotropic displacement parameters and calculated bond-valence sums (BVS) for galeaclolusite.

Atom	Wyck. site	*x*	*y*	*z*	*B* (Å^2)	BVS
As1	8*d*	0.8065	0.0096	0.4689	0.0410(10)	5.26
As2	4*c*	0.8716	¼	0.6675	0.0410(10)	5.38
Al1	8*d*	0.6594	0.0702	0.3315	0.0410(10)	3.16
Al2	8*d*	0.8197	0.098	0.8444	0.0410(10)	3.00
Al3	8*d*	0.7275	0.1683	0.5911	0.0410(10)	2.60
O1	8*d*	0.7299	−0.0049	0.3886	0.0410(10)	2.19
O2	8*d*	0.8685	0.0185	0.3276	0.0410(10)	1.36
O3	8*d*	0.798	0.0881	0.5882	0.0410(10)	2.02
O4	8*d*	0.8205	−0.0626	0.6033	0.0410(10)	1.91
O5	4*c*	0.7918	¼	0.6211	0.0410(10)	2.39
O6	4*c*	0.9328	¼	0.5212	0.0410(10)	1.33
O7	8*d*	0.8817	0.1739	0.7934	0.0410(10)	1.84
OH1	8*d*	0.7206	0.1521	0.3413	0.0410(10)	0.94
OH2	8*d*	0.6571	0.0908	0.5755	0.0410(10)	0.89
OH3	8*d*	0.8900	0.0207	0.8614	0.0410(10)	1.11
OH4	8*d*	0.7415	0.155	0.8431	0.0410(10)	0.97
OH5	4*c*	0.665	¼	0.5878	0.0410(10)	1.00
Ow1	8*d*	0.575	0.1142	0.3206	0.0410(10)	0.57
Ow2	8*d*	0.8205	0.1097	1.0833	0.0410(10)	0.54
*W*1	4*c*	0.502	¼	0.271	0.036(9)	
*W*2	8*d*	0.543	0.1567	0.0425	0.036(9)	
*W*3	4*a*	0	0	0	0.036(9)	
*W*4*	8*d*	0.541	0.298	0.537	0.036(9)	
*W*5	8*d*	0.9837	−0.0243	0.3281	0.036(9)	
*W*6	4*c*	0.7589	¼	0.1064	0.036(9)	

*Occupancy = 50%

Table 5. Polyhedral bond distances in galeaclolusite.

As1−O1	1.664	Al1−O1	1.980	Al3−O3	1.993
As1−O2	1.658	Al1−O4	1.824	Al3−O5	1.942
As1−O3	1.679	Al1−OH1	1.892	Al3−OH1	1.970
As1−O4	1.674	Al1−OH2	1.934	Al3−OH2	1.962
<As−O>	1.669	Al1−OH3	1.890	Al3−OH4	1.994
		Al1−Ow1	1.850	Al3−OH5	1.905
As2−O5	1.666	<Al1−O,OH,Ow>	1.895	<Al3−O,OH>	1.961
As2−O6	1.665				
As2−O7 ×2	1.678	Al2−O1	1.950		
<As2−O>	1.672	Al2−O3	2.047		
		Al2−O7	1.864		
		Al2−OH3	1.954		
		Al2−OH4	1.851		
		Al2−Ow2	1.870		
		<Al2−O,OH,Ow>	1.923		

with the Principal Editor of *Mineralogical Magazine* and is available as Supplementary material (see below).

Discussion

A projection of the crystal structure of galeaclolusite along the 7.8 Å axis is shown in Fig. 5a, where it is compared to the same projection of the bulachite structure in Fig. 5b, showing the higher interlayer H_2O content in the former. Figure 6 shows a view of

https://doi.org/10.1180/mgm.2020.98 Published online by Cambridge University Press

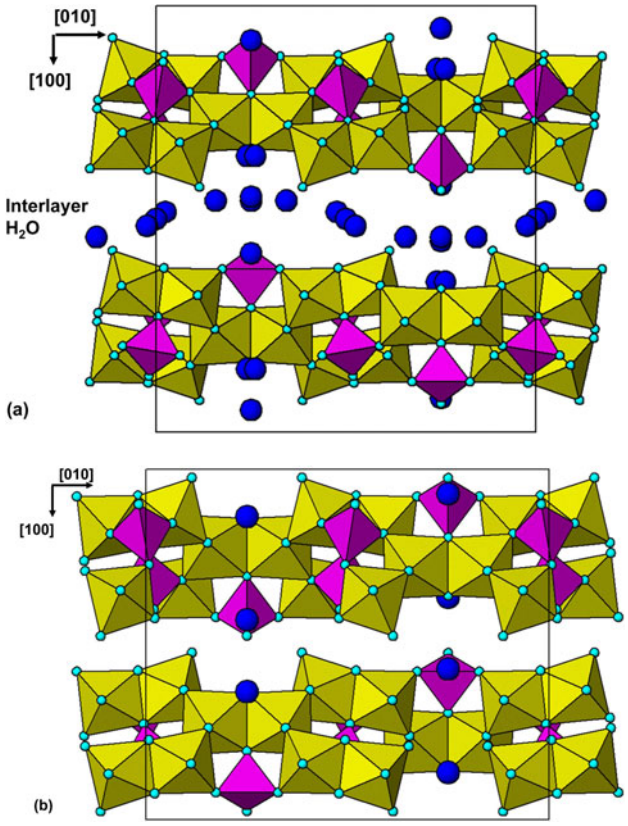

Fig. 5. [001] projection of the layer structure for galeaclolusite (a) compared to bulachite (b). Blue spheres are interlayer water molecules, Al-centred octahedra are yellow and AsO_4 tetrahedra are mauve.

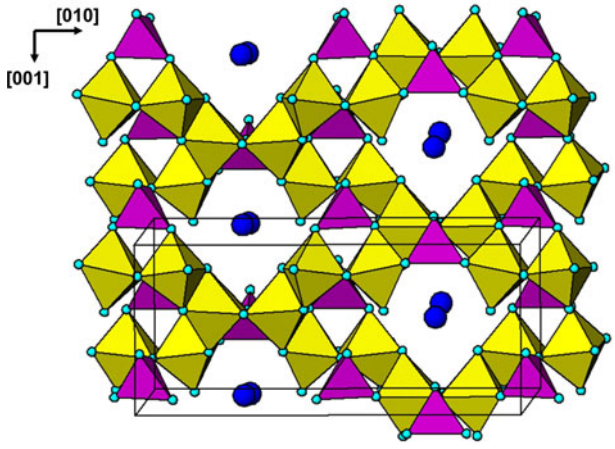

Fig. 6. Projection approximately along [100] of the structure of galeaclolusite, showing spirals along [001] of edge-shared Al-centred octahedra (yellow) and corner-connected AsO_4 tetrahedra (mauve). Blue spheres are H_2O.

the structure normal to the (100) layers. This figure shows that the polyhedral layers are built from edge-shared Al-centred octahedra that form spiral chains along [001], the same as occurs in liskeardite (Grey *et al.*, 2013). The spirals are joined along [010] by edge-sharing of octahedra in the mirror plane at $y = ¼$. The spirals are decorated with AsO_4 tetrahedra that corner-connect to the AlO_6 octahedra in the same manner as in liskeardite.

Table 6. Comparison of galeaclolusite with bulachite.

	Galeaclolusite (present study)	Bulachite* (Grey *et al.*, 2020b)
Ideal formula	$[Al_6(AsO_4)_3(OH)_9{\cdot}(H_2O)_4]{\cdot}8H_2O$	$[Al_6(AsO_4)_3(OH)_9{\cdot}(H_2O)_4]{\cdot}2H_2O$
Symmetry	Orthorhombic, *Pnma*	Orthorhombic, *Pnma*
a (Å)	19.855(4)	15.3994(3)
b (Å)	17.6933(11)	17.6598(3)
c (Å)	7.7799(5)	7.8083(12)
V (Å^3)	2733.0(7)	2123.46(7)
Strongest	9.973, 100 (200)	8.830, 52 (020)
powder	8.851, 60 (020)	7.700, 100 (200)
pattern lines	6.696, 56 (111)	6.964, 40 (101)
d, *I*, (*hkl*)	6.617, 50 (220)	6.479, 72 (111)
	3.506, 74 (122)	5.803, 36 (220)
	3.326, 66 (341)	3.478, 44 (122)
Optics	Biaxial (?)	Biaxial (–)
	$\alpha = 1.550(5)$	$\alpha = 1.540$
	$\gamma = 1.570(5)$	$\beta = 1.546$(calc.)
		$\gamma = 1.548(2)$
		2V(meas.) = 66°

*Optics for bulachite from Walenta (1983).

The composition of the layers is readily established from the refinement using BVS values to distinguish the different anions. The values, in valence units, are given in Table 4. Considering the site multiplicities, they show that the layers contain 12 oxygens, 9 hydroxyls and 4 coordinated H_2O groups per formula unit. This gives the layer formula $Al_6(AsO_4)_3(OH)_9(H_2O)_4$, with $Z = 4$. Adding in the H-bonded H_2O (= *W*) gives the overall formula for galeaclolusite of $Al_6(AsO_4)_3(OH)_9(H_2O)_4]{\cdot}8H_2O$.

Galeaclolusite is closely related to bulachite, differing chemically only in the degree of hydration, and with the structures of both minerals being built from the same heteropolyhedral layers shown in Fig. 5. The properties of the two minerals are compared in Table 6. The ideal formula reported for bulachite from Neubulach, Germany, by Walenta (1983), $Al_6(AsO_4)_3(OH)_9{\cdot}(H_2O)_9$ (scaled by a factor of 3 for comparison), has an H_2O content that is intermediate between that for bulachite from the crystal structure (Grey *et al.*, 2020b) and for galeaclolusite. This is consistent with our XRD study of the Neubulach type specimen that showed it comprised a mixture of the two minerals (Grey *et al.*, 2020b). Bulachite–galeaclolusite intergrowths were also observed on specimens from Sa Malesa, Sardinia, Italy; it is thus possible that both minerals are likely to be found together at all mineral localities where bulachite has been reported.

Acknowledgements. Thanks to Cameron Davidson for EMP sample preparation and to Vincent Bourgoin, Association Jean Wyart, Paris for the images shown in Figs 1 and 2. Part of this research was undertaken at the powder diffraction beamline at the Australian Synchrotron, Victoria, Australia and we thank Anita D'Angelo for help with the data collection.

Supplementary material. To view supplementary material for this article, please visit https://doi.org/10.1180/mgm.2020.98

References

Favreau G. and Galea-Clolus V. (2014) *Cap Garonne*. Association Française de Microminéralogie, Carry-le-Rouet, France.

Frau F. and Da Pelo S. (2001) Bulachite, a rare aluminium arsenate from Sardinia, Italy: the second world occurrence. *Neues Jahrbuch für Mineralogie, Monatshafte*, **2001**, 18–26.

Gagné O.C. and Hawthorne F.C. (2015) Comprehensive derivation of bond-valence parameters for ion pairs involving oxygen. *Acta Crystallographica*, **B71**, 562–578.

Grey I.E., Mumme W.G., MacRae C.M., Caradoc-Davies. T., Price J.R., Rumsey M.S. and Mills S.J. (2013) Chiral edge-shared octahedral chains in liskeardite, $[(Al,Fe)_{32}(AsO_4)_{18}(OH)_{42}(H_2O)_{22}]\cdot 52H_2O$, an open framework mineral with a pharmacoalumite-related structure. *Mineralogical Magazine*, **77**, 3125–3135.

Grey I.E., Mumme W.G., Price J.R., Mills S.J., MacRae C.M. and Favreau G. (2014) Ba-Cu ordering in bariopharmacoalumite-*Q2a2b2c* from Cap Garonne, France. *Mineralogical Magazine*, **78**, 851–860.

Grey I.E., Brand H.E.A. and Betterton J. (2016) Dehydration phase transitions in new aluminium arsenate minerals from the Penberthy Croft mine, Cornwall, UK. *Mineralogical Magazine*, **80**, 1205–1217.

Grey I.E., Favreau G., Mills S.J., Mumme W.G., Bougerol C., Brand H.E.A., Kampf A.R., MacRae C.M. and Shanks, F. (2020a) Galeaclolusite, IMA 2020-052, in: CNMNC Newsletter 58, *Mineralogical Magazine*, 84, https://doi.org/10.1180/mgm.2020

Grey I.E., Yoruk E., Kodjikian S., Klein H., Bougerol C., Brand H.E.A., Bordet P., Mumme W.G., Favreau G. and Mills S.J. (2020b) Bulachite, $[Al_6(AsO_4)_3\ (OH)_9(H_2O)_4]\cdot 2H_2O$ from Cap Garonne, France: Crystal structure and formation from a higher hydrate. *Mineralogical Magazine*, **84**, 608–615.

Libowitzky E. (1999) Correlation of O-H stretching frequencies and O–H···O hydrogen bond lengths in minerals. *Monatsche fur Chemie*, **130**, 1047–1059.

Mandarino J.A. (2007) The Gladstone-Dale compatibility of minerals and its use for selecting mineral species for further study. *The Canadian Mineralogist*, **45**, 1307–1324.

Mills S.J., Christy A.G., Schnyder C., Favreau G. and Price J.R. (2014) The crystal structure of camerolaite and structural variation in the cyanotrichite family of merotypes. *Mineralogical Magazine*, **78**, 1527–1552.

Mills S.J., Christy A.G., Colombo F. and Price J.R. (2015) The crystal structure of cyanotrichite. *Mineralogical Magazine*, **79**, 321–335.

Mills S.J., Christy A.G., Favreau G. and Galea-Clolus V. (2017) Multidimensional structural variation in the cyanotrichite family of merotypes: camerolaite-3*b*-*F*-1. *Acta Crystallographica*, **B73**, 950–955.

Mills S.J., Christy A.G. and Favreau G. (2018) The crystal structure of ceruleite, $CuAl_4[AsO_4]_2(OH)_8(H_2O)_4$, from Cap Garonne, France. *Mineralogical Magazine*, **82**, 181–187.

Mills S.J., Missen O.P. and Favreau G. (2019) The crystal structure of Ni-rich gordaite-thérèsemagnanite from Cap Garonne, France. *Mineralogical Magazine*, **83**, 459–463.

Mills S.J., Kolitsch U., Favreau G., Birch W.D., Galea-Clolus V. and Henrich J.M. (2020) Gobelinite, the Co analogue of ktenasite from Cap Garonne, France, and Eisenzecher Zug, Germany. *European Journal of Mineralogy*, **32**, 637–644.

Myeni S.C.B., Traina S.J., Waychunas G.A. and Logan T.J. (1998) Experimental and theoretical vibrational spectroscopic evaluation of arsenate coordination in aqueous solutions, solids and at mineral–water interfaces. *Geochimica Cosmochimica Acta*, **62**, 3285–3300.

Petříček V., Dušek M. and Palatinus L. (2014) Crystallographic Computing System JANA2006: General features. *Zeitschrift für Kristalloraphie*, **229**, 345–352.

Pouchou J. (1993) PAP – X-ray microanalysis of stratified specimens. *Analytical Chimica Acta*, **283**, 81–97.

Plášil J., Petříček V., Mills S. J., Favreau G. and Galea-Clolus V. (2018) Zippeite from Cap Garonne, France: an example of reticular twinning. *Zeitschrift für Kristallographie – Crystalline Materials*, **233**, 861–865.

Sarp H. and Chiappero P. J. (1992) Deloryite, $Cu_4(UO_2)(MoO_4)_2(OH)_6$, a new mineral from the Cap Garonne mine near Le Pradet, Var, France. *Neues Jahrbuch für Mineralogie, Monatshefte*, **1992**, 58–64.

Schafer D., Donn M., Atteia O., MacRae C., Raven M., Pejcic B. and Prommer H. (2018) Fluoride and phosphate release from carbonate-rich fluorapatite during managed aquifer recharge. *Journal of Hydrology*, **562**, 809–820.

Walenta K. (1983) Bulachit, ein neues Aluminiumarsenatmineral von Neubulach im nördlichen Schwarzwald. *Aufschluss*, **34**, 445–451.

https://doi.org/10.1180/mgm.2020.98 Published online by Cambridge University Press